16. Nanomechanical Cantilever Array Sensors

Microfabricated cantilever sensors have attracted much interest in recent years as devices for the fast and reliable detection of small concentrations of molecules in air and solution. In addition to application of such sensors for gas and chemical-vapor sensing, for example as an artificial nose, they have also been employed to measure physical properties of tiny amounts of materials in miniaturized versions of conventional standard techniques such as calorimetry, thermogravimetry, weighing, photothermal spectroscopy, as well as for monitoring chemical reactions such as catalysis on small surfaces. In the past few years, the cantilever-sensor concept has been extended to biochemical applications and as an analytical device for measurements of biomaterials. Because of the label-free detection principle of cantilever sensors, their small size and scalability, this kind of device is advantageous for diagnostic applications and disease monitoring, as well as for genomics or proteomics purposes. The use of microcantilever arrays enables detection of several analytes simultaneously and solves the inherent problem of thermal drift often present when using single microcantilever sensors, as some of the cantilevers can be used as sensor cantilevers for detection, and other cantilevers serve as passivated reference cantilevers that do not exhibit affinity to the molecules to be detected.

16.1 Technique

Sensors are devices that detect, or sense, a signal. Moreover, a sensor is also a transducer, i. e. it transforms one form of energy into another or responds to a physical parameter. Most people will associate sensors with electrical or electronic devices that produce a change in response when an external physical parameter is changed. However, many more types of transducers exist, such as electrochemical (pH probe), electromechanical (piezoelectric actuator, quartz, strain gauge), electroacoustic (gramophone pickup, microphone), photoelectric (photodiode, solar cell), electromagnetic (antenna), magnetic (Hall-effect sensor, tape or hard-disk head for storage applications), electrostatic (electrometer), thermoelectric (thermocouple, thermoresistors), and electrical (capacitor, resistor). Here we want to concentrate on a further type of sensor not yet mentioned: the mechanical sensor. It responds to changes of an external parameter, such as temperature changes or molecule adsorption, by a mechanical response, e.g. by bending or deflection.

16.1.1 Cantilevers

Mechanical sensors consist of a fixed and a movable part. The movable part can be a thin membrane, a plate or a beam, fixed at one or both ends. The structures described here are called cantilevers. A cantilever is regarded here as a microfabricated rectangular bar-shaped structure that is longer than it is wide and has a thickness that is much smaller than its length or width. It is a horizontal structural element supported only at one end on a chip body; the other end is free (Fig. 16.1). Most often it is used as a mechanical probe to image the topography of a sample using a technique called atomic force microscopy (AFM) or scanning force microscopy (SFM) [16.1], invented by *Binnig*, *Quate* and *Gerber* in the mid 1980s [16.1]. For AFM a microfabricated sharp tip is attached to the apex of the cantilever and serves as a local probe to scan the sample surface. The distance between tip and surface is controlled via sensitive measurement of interatomic forces in the piconewton range.

By scanning the tip across a conductive or nonconductive surface using an x-y-z actuator system (e.g. a piezoelectric scanner), an image of the topography is obtained by recording the correction signal that has to be applied to the z-actuation drive to keep the interaction between tip and sample surface constant. SFM methods are nowadays well established in scientific research, education and, to a certain extent, also in industry. Beyond imaging of surfaces, cantilevers have been used for many other purposes. However, here we focus on their application as sensor devices.

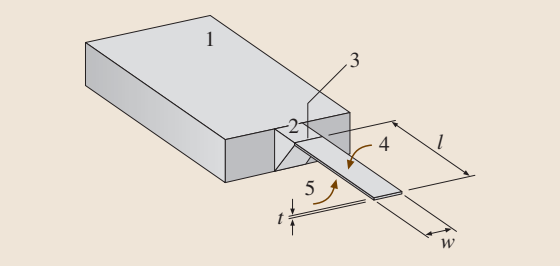

Fig. 16.1 Schematic of a cantilever: (1) rigid chip body, (2) solid cantilever-support structure, (3) hinge of cantilever, (4) upper surface of the cantilever, which is usually functionalized with a sensor layer for detection of molecules, (5) lower surface of the cantilever, usually passivated in order not to show affinity to the molecules to be detected. The geometrical dimensions, length l, width w and thickness t, are indicated

16.1.2 History of Cantilever Sensors

The idea of using beams of silicon as sensors to measure deflections or changes in resonance frequency is actually quite old. First reports go back to 1968, when *Wilfinger* et al. [16.2] investigated silicon cantilever structures of 50 mm × 30 mm × 8 mm, i. e. quite large structures, for detecting resonances. On the one hand, they used localized thermal expansion in diffused resistors (piezoresistors) located near the cantilever support to create a temperature gradient for actuating the cantilever at its resonance frequency. On the other hand, the piezoresistors could also be used to sense mechanical deflection of the cantilever. This early report already contains concepts for sensing and actuation of cantilevers. In the following years only a few reports are available on the use of cantilevers as sensors, e.g. *Heng* [16.3], who fabricated gold cantilevers capacitively coupled to microstrip lines in 1971 to mechanically trim high-frequency oscillator circuits. In 1979, *Petersen* [16.4] constructed cantilever-type micromechanical membrane switches in silicon that should have filled the gap between silicon transistors and mechanical electromagnetic relays. *Kolesar* [16.5] suggested the use of cantilever structures as electronic nerve-agent detectors in 1985.

Only with the availability of microfabricated cantilevers for AFM [16.1] did reports on the use of cantilevers as sensors become more frequent. In 1994, *Itoh* et al. [16.6] presented a cantilever coated with a thin film of zinc oxide and proposed piezoresistive deflection readout as an alternative to optical beam-deflection readout. *Cleveland* et al. [16.7] reported the tracking of cantilever resonance frequency to detect nanogram changes in mass loading when small particles are deposited onto AFM probe tips. *Thundat* et al. [16.8] showed that the resonance frequency as well as static bending of microcantilevers are influenced by ambient conditions, such as moisture adsorption, and that deflection of metal-coated cantilevers can be further influenced by thermal effects (bimetallic effect). The first chemical sensing applications were presented by *Gimzewski* et al. [16.9], who used static cantilever bending to detect chemical reactions with very high sensitivity. Later *Thundat* et al. [16.10] observed changes in the resonance frequency of microcantilevers due to adsorption of analyte vapor on exposed surfaces. Frequency changes have been found to be caused by mass loading or adsorption-induced changes in the cantilever spring constant. By coating cantilever surfaces with hygroscopic materials, such as phosphoric acid or gelatin, the

cantilever can sense water vapor with picogram mass resolution.

The deflection of individual cantilevers can easily be determined using AFM-like optical beam-deflection electronics. However, single cantilever responses can be prone to artifacts such as thermal drift or unspecific adsorption. For this reason the use of passivated reference cantilevers is desirable. The first use of cantilever arrays with sensor and reference cantilevers was reported in 1998 [16.11], and represented significant progress for the understanding of true (difference) cantilever responses.

16.2 Cantilever Array Sensors

16.2.1 Concept

For the use of a cantilever as a sensor, neither a sharp tip at the cantilever apex nor a sample surface is required. The cantilever surfaces serve as sensor surfaces and allow the processes taking place on the surface of the beam to be monitored with unprecedented accuracy, in particular the adsorption of molecules. The formation of molecule layers on the cantilever surface will generate surface stress, eventually resulting in a bending of the cantilever, provided the adsorption preferentially occurs on one surface of the cantilever. Adsorption is controlled by coating one surface (typically the upper surface) of a cantilever with a thin layer of a material that exhibits affinity to molecules in the environment (sensor surface). This surface of the cantilever is referred to as the functionalized surface. The other surface of the cantilever (typically the lower surface) may be left uncoated or be coated with a passivation layer, i. e. a chemical surface that does not exhibit significant affinity to the molecules in the environment to be detected. To enable functionalized surfaces to be established, often a metal layer is evaporated onto the surface designed as sensor surface. Metal surfaces, e.g. gold, may be used to covalently bind a monolayer that represents the chemical surface sensitive to the molecules to be detected from environment. Frequently, a monolayer of thiol molecules covalently bound to a gold surface is used. The gold layer is also favorable for use as a reflection layer if the bending of the cantilever is read out via an optical beam-deflection method.

16.2.2 Compressive and Tensile Stress

Given a cantilever coated with gold on its upper surface for adsorption of alkanethiol molecules and left uncoated on its lower surface (consisting of silicon and silicon oxide), the adsorption of thiol molecules will take place on the upper surface of the cantilever, resulting in a downward bending of the cantilever due to the formation of surface stress. We will call this process development of compressive surface stress, because the forming self-assembled monolayer produces a downward bending of the cantilever (away from the gold coating). In the opposite situation, i. e. when the cantilever bends upwards, we would speak of tensile stress. If both the upper and lower surfaces of the cantilevers are involved in the reaction, then the situation will be much more complex, as a predominant compressive stress formation on the lower cantilever surface might appear like tensile stress on the upper surface. For this reason, it is of utmost importance that the lower cantilever surface is passivated in order that ideally no processes take place on the lower surface of the cantilever.

16.2.3 Disadvantages of Single Microcantilevers

Single microcantilevers are susceptible to parasitic deflections that may be caused by thermal drift or chemical interaction of a cantilever with its environment, in particular if the cantilever is operated in a liquid. Often, a baseline drift is observed during static-mode measurements. Moreover, nonspecific physisorption of molecules on the cantilever surface or nonspecific binding to receptor molecules during measurements may contribute to the drift.

16.2.4 Reference and Sensor Cantilevers in an Array

To exclude such influences, simultaneous measurement of reference cantilevers aligned in the same array as the sensing cantilevers is crucial [16.11]. As the difference in signals from the reference and sensor cantilevers shows the net cantilever response, even small sensor responses can be extracted from large cantilever deflections without being dominated by undesired effects. When only single microcantilevers are used, no thermal-drift compensation is possible. To obtain useful data under these circumstances, both microcantilever surfaces have to be chemically well defined. One of the

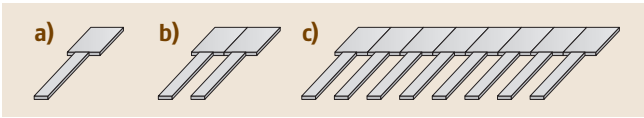

Fig. 16.2 (**a**) Single cantilever; (**b**) a pair of cantilevers, one to be used as a sensor cantilever, the other as a reference cantilever, and (**c**) an array of cantilevers with several sensor and reference cantilevers

surfaces, typically the lower one, has to be passivated; otherwise the cantilever response will be convoluted with undesired effects originating from uncontrolled reactions taking place on the lower surface (Fig. 16.2a). With a pair of cantilevers, reliable measurements are obtained. One cantilever is used as the sensor cantilever (typically coated on the upper side with a molecule layer exhibiting affinity to the molecules to be detected), whereas the other cantilever serves as the reference cantilever. It should be coated with a passivation layer on the upper surface so as not to exhibit affinity to the molecules to be detected. Thermal drifts are canceled out if difference responses, i. e. difference in deflections of sensor and reference cantilevers, are taken. Alternatively, both cantilevers are used as sensor cantilevers (sensor layer on the upper surfaces), and the lower surface has to be passivated (Fig. 16.2b). It is best to use a cantilever array (Fig. 16.2c), in which several cantilevers are used either as sensor or as reference cantilevers so that multiple difference signals can be evaluated simultaneously. Thermal drift is canceled out as one surface of all cantilevers, typically the lower one, is left uncoated or coated with the same passivation layer.

16.3 Modes of Operation

In analogy to AFM, various operating modes for cantilevers are described in the literature. The measurement of static deflection upon the formation of surface stress during adsorption of a molecular layer is termed the *static mode*. *Ibach* used cantilever-like structures to study adsorbate-induced surface stress [16.12] in 1994. Surface-stress-induced bending of cantilevers during the adsorption of alkanethiols on gold was reported by *Berger* et al. in 1997 [16.13]. The mode corresponding to noncontact AFM, termed the *dynamic mode*, in which a cantilever is oscillated at its resonance frequency, was described by *Cleveland* et al. [16.7]. They calculated mass changes from shifts in the cantilever resonance frequency upon the mounting of tiny tungsten particle spheres at the apex of the cantilever. The so-called *heat mode* was pioneered by *Gimzewski* et al. [16.9], who took advantage of the bimetallic effect that produces a bending of a metal-coated cantilever when heat is produced on its surface. Therewith they constructed a miniaturized calorimeter with picojoule sensitivity. Further operating modes exploit other physical effects such as the production of heat from the absorption of light by materials deposited on the cantilever (photothermal spectroscopy) [16.14], or cantilever bending caused by electric or magnetic forces.

16.3.1 Static Mode

The continuous bending of a cantilever with increasing coverage by molecules is referred to as operation in the static mode, see Fig. 16.3a. Adsorption of molecules onto the functional layer produces stress at the interface between the functional layer and the molecular layer forming. Because the forces within the functional layer try to keep the distance between molecules constant, the cantilever beam responds by bending because of its extreme flexibility. This property is described by the spring constant k of the cantilever, which for a rectangular microcantilever of length l, thickness t and width w is calculated as

$$k = \frac{Ewt^3}{4l^3} , \tag{16.1}$$

where E is the Young's modulus [$E_{\mathrm{Si}} = 1.3 \times 10^{11}\,\mathrm{N/m^2}$ for Si(100)].

As a response to surface stress, e.g. owing to adsorption of a molecular layer, the microcantilever bends, and its shape can be approximated as part of a circle with radius R. This radius of curvature is given by [16.15, 16]

$$\frac{1}{R} = \frac{6(1-\nu)}{Et^2} . \tag{16.2}$$

The resulting surface stress change is described using Stoney's formula [16.15]

$$\Delta\sigma = \frac{Et^2}{6R(1-\nu)} , \tag{16.3}$$

where E is Young's modulus, t the thickness of the cantilever, ν the Poisson's ratio ($\nu_{\mathrm{Si}} = 0.24$), and R the bending radius of the cantilever.

Static-mode operation has been reported in various environments. In its simplest configuration, molecules

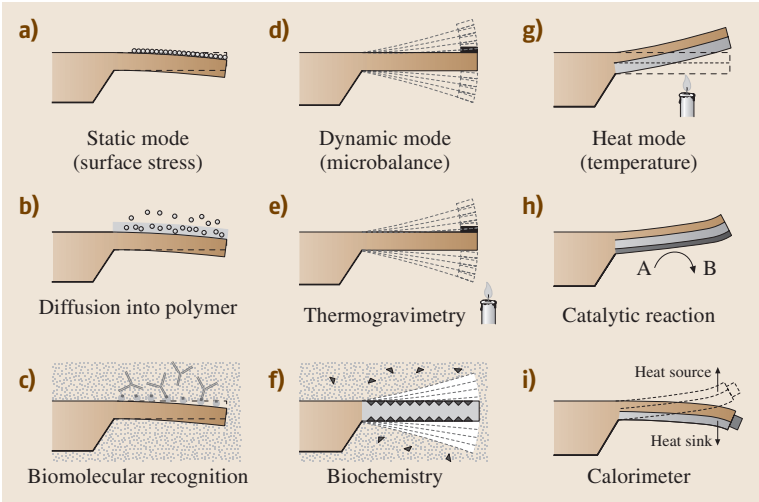

Fig. 16.3a–i Basic cantilever operation modes: **(a)** static bending of a cantilever on adsorption of a molecular layer. **(b)** Diffusion of molecules into a polymer layer leads to swelling of the polymer and eventually to a bending of the cantilever. **(c)** Highly specific molecular recognition of biomolecules by receptors changes the surface stress on the upper surface of the cantilever and results in bending. **(d)** Oscillation of a cantilever at its resonance frequency (dynamic mode) allows information on mass changes taking place on the cantilever surface to be obtained (application as a microbalance). **(e)** Changing the temperature while a sample is attached to the apex of the cantilever allows information to be gathered on decomposition or oxidation process. **(f)** Dynamic-mode measurements in liquids yield details on mass changes during biochemical processes. **(g)** In the heat mode, a bimetallic cantilever is employed. Here bending is due to the difference in the thermal expansion coefficients of the two materials. **(h)** A bimetallic cantilever with a catalytically active surface bends due to heat production during a catalytic reaction. **(i)** A tiny sample attached to the apex of the cantilever is investigated, taking advantage of the bimetallic effect.Tracking the deflection as a function of temperature allows the observation of phase transitions in the sample in a calorimeter mode

from the gaseous environment adsorb on the functionalized sensing surface and form a molecular layer (Fig. 16.3a), provided the molecules exhibit some affinity to the surface. In the case of alkanethiol covalently binding to gold, the affinity is very high, resulting in a fast bending response within minutes [16.13]. Polymer sensing layers only exhibit a partial sensitivity, i. e. polymer-coated cantilevers always respond to the presence of volatile molecules, but the magnitude and temporal behavior are specific to the chemistry of the polymer. Molecules from the environment diffuse into the polymer layer at different rates, mainly depending on the size and solubility of the molecules in the polymer layer (Fig. 16.3b). A wide range of hydrophilic/hydrophobic polymers can be selected, differing in their affinity to polar/unpolar molecules. Thus, the polymers can be chosen according to what an application requires.

Static-mode operation in liquids, however, usually requires rather specific sensing layers, based on molecular recognition, such as DNA hybridization [16.17] or antigen–antibody recognition (Fig. 16.3c). Cantilevers functionalized by coating with biochemical sensing layers respond very specifically using biomolecular key–lock principles of molecular recognition. However, whether molecular recognition will actually lead to a bending of the cantilever depends on the efficiency of transduction, because the surface stress has to be generated very close to the cantilever surface to produce bending. By just scaling down standard gene-chip strategies to cantilever geometry utilizing long spacer molecules so that DNA molecules become more accessible for hybridization, the hybridization takes place at a distance of several nanometers from the cantilever surface. In such experiments, no cantilever bending was observed [16.18].

16.3.2 Dynamic Mode

Mass changes can be determined accurately by using a cantilever actuated at its eigenfrequency. The

eigenfrequency is equal to the resonance frequency of an oscillating cantilever if the elastic properties of the cantilever remain unchanged during the molecule-adsorption process and if damping effects are insignificant. This mode of operation is called the dynamic mode (e.g., the use as a microbalance, Fig. 16.3d). Owing to mass addition on the cantilever surface, the cantilever's eigenfrequency will shift to a lower value. The frequency change per mass change on a rectangular cantilever is calculated [16.19] according to

$$\Delta f/\Delta m = \frac{1}{4\pi n_l l^3 w} \times \sqrt{\frac{E}{\rho^3}}\,, \tag{16.4}$$

where $\rho = m/lwt$ is the mass density of the microcantilever and the deposited mass, and $n_l \approx 1$ is a geometrical factor.

The mass change is calculated [16.8] from the frequency shift using

$$\Delta m = \frac{k}{4\pi^2} \times \left(\frac{1}{f_1^2} - \frac{1}{f_0^2}\right)\,, \tag{16.5}$$

where f_0 is the eigenfrequency before the mass change occurs, and f_1 the eigenfrequency after the mass change.

Mass-change determination can be combined with varying environment temperature conditions (Fig. 16.3e) to obtain a method introduced in the literature as *micromechanical thermogravimetry* [16.20]. A tiny piece of sample to be investigated has to be mounted at the apex of the cantilever. Its mass should not exceed several hundred nanograms. Adsorption, desorption and decomposition processes, occurring while changing the temperature, produce mass changes in the picogram range that can be observed in real time by tracking the resonance-frequency shift.

Dynamic-mode operation in a liquid environment is more difficult than in air, because of the large damping of the cantilever oscillation due to the high viscosity of the surrounding media (Fig. 16.3f). This results in a low quality factor Q of the oscillation, and thus the resonance frequency shift is difficult to track with high resolution. The quality factor is defined as

$$Q = 2\Delta f/f_0\,. \tag{16.6}$$

Whereas in air the resonance frequency can easily be determined with a resolution of below 1 Hz, only a frequency resolution of about 20 Hz is expected for measurements in a liquid environment.

The damping or altered elastic properties of the cantilever during the experiment, e.g. by a stiffening or softening of the spring constant caused by the adsorption of a molecule layer, result in the fact that the measured resonance frequency will not be exactly equal to the eigenfrequency of the cantilever, and therefore the mass derived from the frequency shift will be inaccurate. In a medium, the vibration of a cantilever is described by the model of a driven damped harmonic oscillator:

$$m^* \frac{\mathrm{d}^2 x}{\mathrm{d}t^2} + \gamma \frac{\mathrm{d}x}{\mathrm{d}t} + kx = F\cos(2\pi ft)\,, \tag{16.7}$$

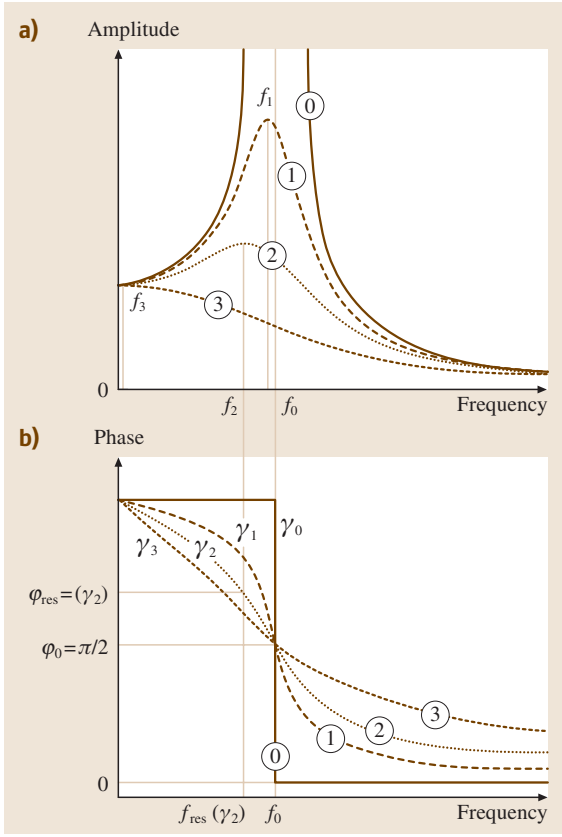

Fig. 16.4 **(a)** Resonance curve with no damping (0), and increasing damping (1)–(3). The undamped curve with resonance frequency f_0 exhibits a very high amplitude, whereas the resonance peak amplitude decreases with damping. This also involves a shift in resonance frequencies from f_1 to f_3 to lower values. **(b)** Corresponding phase curves showing no damping (0), and increasing damping (1)–(3). The step-like phase jump at resonance of the undamped resonance gradually broadens with increasing damping

where $m^* = \text{const}(m_c + m_l)$ is the effective mass of the cantilever (for a rectangular cantilever the constant is 0.25). Especially in liquids, the mass of the co-moved liquid m_l adds significantly to the mass of the cantilever m_c. The term $\gamma \frac{dx}{dt}$ is the drag force due to damping, $F\cos(2\pi ft)$ is the driving force executed by the piezo-oscillator, and k is the spring constant of the cantilever.

If no damping is present, the eigenfrequencies of the various oscillation modes of a bar-shaped cantilever are calculated according to

$$f_n = \frac{\alpha_n^2}{2\pi}\sqrt{\frac{k}{2(m_c + m_l)}}\,, \tag{16.8}$$

where f_n are the eigenfrequencies of the n-th mode, α_n are constants depending on the mode: $\alpha_1 = 1.8751, \alpha_2 = 4.6941, \alpha_n = \pi(n - 0.5)$; k is the spring constant of the cantilever, m_c the mass of the cantilever, and m_l the mass of the medium surrounding the cantilever, e.g. liquid [16.21].

Addition of mass to the cantilever due to adsorption will change the effective mass as follows:

$$m^* = \text{const}(m_c + m_l + \Delta m)\,, \tag{16.9}$$

where Δm is the additional mass adsorbed. Typically, the co-moved mass of the liquid is much larger than the adsorbed mass.

Figure 16.4 clearly shows that the resonance frequency is only equal to the eigenfrequency if no damping is present. With damping, the frequency at which the peak of the resonance curve occurs is no longer identical to that at which the turning point of the phase curve occurs. For example, resonance curve 2 with damping γ_2 has its maximum amplitude at frequency f_2. The corresponding phase would be $\varphi_{res}(\gamma_2)$, which is not equal to $\pi/2$, as would be expected in the undamped case. If direct resonance-frequency tracking or a phase-locked loop is used to determine the frequency of the oscillating cantilever, then only its resonance frequency is detected, but not its eigenfrequency. Remember that the eigenfrequency, and not the resonance frequency, is required to determine mass changes.

16.3.3 Heat Mode

If a cantilever is coated with metal layers, thermal expansion differences in the cantilever and the coating layer will further influence cantilever bending as a function of temperature. This mode of operation is referred to as the *heat mode* and causes cantilever bending because of differing thermal expansion coefficients in the sensor layer and cantilever materials [16.9] (Fig. 16.3g):

$$\Delta z = \frac{5}{4}(\alpha_1 - \alpha_2)\frac{t_1 + t_2}{t_2^2\kappa}\frac{l^3}{(\lambda_1 t_1 + \lambda_2 t_2)w}P\,. \tag{16.10}$$

Here α_1, α_2 are the thermal expansion coefficients of the cantilever and coating materials, respectively, λ_1, λ_2 their thermal conductivities, t_1, t_2 the material thicknesses, P is the total power generated on the cantilever, and κ is a geometry parameter of the cantilever device.

Heat changes are either caused by external influences (change in temperature, Fig. 16.3g), occur directly on the surface by exothermal, e.g. catalytic, reactions (Fig. 16.3h), or are due to material properties of a sample attached to the apex of the cantilever (micromechanical calorimetry, Fig. 16.3i). The sensitivity of the cantilever heat mode is orders of magnitude higher than that of traditional calorimetric methods performed on milligram samples, as it only requires nanogram amounts of sample and achieves nanojoule [16.20], picojoule [16.22] and femtojoule [16.23] sensitivity.

These three measurement modes have established cantilevers as versatile tools to perform experiments in nanoscale science with very small amounts of material.

16.3.4 Further Operation Modes

Photothermal Spectroscopy

When a material adsorbs photons, a fraction of the energy is converted into heat. This photothermal heating can be measured as a function of the light wavelength to provide optical absorption data of the material. The interaction of light with a bimetallic microcantilever creates heat on the cantilever surface, resulting in a bending of the cantilever [16.14]. Such bimetallic-cantilever devices are capable of detecting heat flows due to an optical heating power of 100 pW, which is two orders of magnitude better than in conventional photothermal spectroscopy.

Electrochemistry

A cantilever coated with a metallic layer (measurement electrode) on one side is placed in an electrolytic medium, e.g. a salt solution, together with a metallic reference electrode, usually made of a noble metal. If the voltage between the measurement and the reference electrode is changed, electrochemical processes

on the measurement electrode (cantilever) are induced, such as adsorption or desorption of ions from the electrolyte solution onto the measurement electrode. These processes lead to a bending of the cantilever due to changes in surface stress and in the electrostatic forces [16.24].

Detection of Electrostatic and Magnetic Forces

The detection of electrostatic and magnetic forces is possible if charged or magnetic particles are deposited on the cantilever [16.25, 26]. If the cantilever is placed in the vicinity of electrostatic charges or magnetic particles, attractive or repulsion forces occur according to the polarity of the charges or magnetic particles present on the cantilever. These forces will result in an upward or a downward bending of the cantilever. The magnitude of the bending depends on the distribution of charged or magnetic particles on both the cantilever and in the surrounding environment according to the laws of electrostatics and magnetism.

16.4 Microfabrication

Silicon cantilever sensor arrays have been microfabricated using a dry-etching silicon-on-insulator (SOI) fabrication technique developed in the micro-/nanomechanics department at the IBM Zurich Research Laboratory. One chip comprises eight cantilevers, having a length of 500 μm, a width of 100 μm, and a thickness of 0.5 μm, and arranged on a pitch of 250 μm. For dynamic-mode operation, the cantilever thickness may be up to 7 μm. The resonance frequencies of the cantilevers vary by 0.5% only, demonstrating the high reproducibility and precision of cantilever fabrication. A scanning electron microscopy image of a cantilever sensor-array chip is shown in Fig. 16.5.

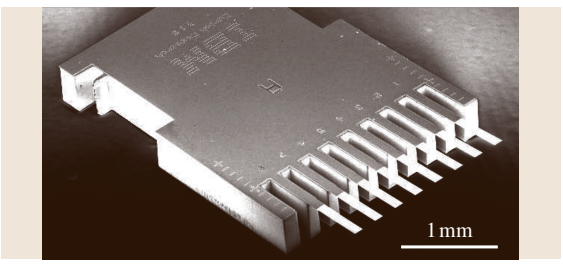

Fig. 16.5 Scanning electron micrograph of a cantilever-sensor array. Image courtesy of Viola Barwich, University of Basel, Switzerland

16.5 Measurement Set-Up

16.5.1 Measurements in Gaseous or Liquid Environments

A measurement set-up for cantilever arrays consists of four major parts: (1) the measurement chamber containing the cantilever array, (2) an optical or electrical system to detect the cantilever deflection (e.g. laser sources, collimation lenses and a position-sensitive detector (PSD), or piezoresistors and Wheatstone-bridge detection electronics), (3) electronics to amplify, process and acquire the signals from the detector, and (4) a gas- or liquid-handling system to inject samples reproducibly into the measurement chamber and purge the chamber.

Figure 16.6 shows the schematic set-up for experiments performed in a gaseous (Fig. 16.6(a)) and a liquid, biochemical (Fig. 16.6(b)) environment for the optical beam-deflection embodiment of the measurement set-up. The cantilever sensor array is located in an analysis chamber with a volume of 3–90 μl, which has inlet and outlet ports for gases or liquids. The cantilever deflection is determined by means of an array of eight vertical-cavity surface-emitting lasers (VCSELs) arranged at a linear pitch of 250 μm that emit at a wavelength of 760 nm into a narrow cone of 5 to 10°.

The light of each VCSEL is collimated and focused onto the apex of the corresponding cantilever by a pair of achromatic doublet lenses, 12.5 mm in diameter. This size has to be selected in such a way that all eight laser beams pass through the lens close to its center to minimize scattering, chromatic and spherical aberration artifacts. The light is then reflected off the gold-coated surface of the cantilever and hits the surface of a position-sensing detector (PSD). PSDs are light-sensitive photo-potentiometer-like devices that produce photocurrents at two opposing electrodes. The magnitude of the photocurrents depends linearly on the distance of the

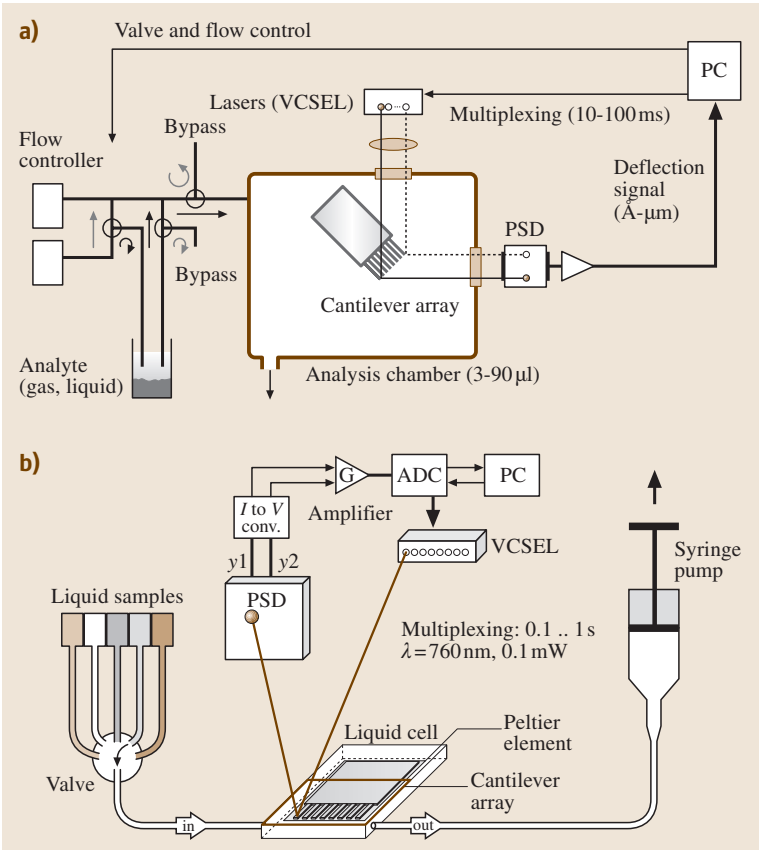

Fig. 16.6 Schematic of measurement set-ups for **(a)** a gaseous (artificial nose) and **(b)** a liquid environment (biochemical sensor)

impinging light spot from the electrodes. Thus the position of an incident light beam can easily be determined with micrometer precision. The photocurrents are transformed into voltages and amplified in a preamplifier. As only one PSD is used, the eight lasers cannot be switched on simultaneously. Therefore, a time-multiplexing procedure is used to switch the lasers on and off sequentially at typical intervals of 10–100 ms. The resulting deflection signal is digitized and stored together with time information on a personal computer (PC), which also controls the multiplexing of the VCSELs as well as the switching of the valves and mass flow controllers used for setting the composition ratio of the analyte mixture.

The measurement set-up for liquids (Fig. 16.6b) consists of a poly-etheretherketone (PEEK) liquid cell, which contains the cantilever array and is sealed by a viton O-ring and a glass plate. The VCSELs and the PSD are mounted on a metal frame around the liquid cell. After preprocessing the position of the deflected light beam in a current-to-voltage converter and amplifier stage, the signal is digitized in an analog-to-digital converter and stored on a PC. The liquid cell is equipped with inlet and outlet ports for liquids. They are connected via 0.18-mm-inner-diameter Teflon tubing to individual thermally equilibrated glass containers, in which the biochemical liquids are stored. A six-position valve allows the inlet to the liquid chamber to be connected to each of the liquid-sample containers separately. The liquids are pulled (or pushed) through the liquid chamber by means of a syringe pump connected to the outlet of the chamber. A Peltier element is situated very close to the lumen of the chamber to allow temperature regulation within the chamber. The entire experimental set-up is housed in a temperature-controlled box regulated with an accuracy of 0.01 K to the target temperature.

16.5.2 Readout Principles

This section describes various ways to determine the deflection of cantilever sensors. They differ in sensitivity,

effort for alignment and set-up, robustness and ease of readout as well as their potential for miniaturization.

Piezoresistive readout

Piezoresistive cantilevers [16.6, 20] are usually U-shaped, having diffused piezoresistors in both of the legs close to the hinge (Fig. 16.7a). The resistance in the piezoresistors is measured by a Wheatstone-bridge technique employing three reference resistors, one of which is adjustable. The current flowing between the two branches of the Wheatstone bridge is initially nulled by changing the resistance of the adjustable resistor. If the cantilever bends, the piezoresistor changes its value and a current will flow between the two branches of the Wheatstone bridge. This current is converted via a differential amplifier into a voltage for static-mode measurement. For dynamic-mode measurement, the piezoresistive cantilever is externally actuated via a frequency generator connected to a piezocrystal. The alternating current (AC) actuation voltage is fed as reference voltage into a lock-in amplifier and compared with the response of the Wheatstone-bridge circuit. This technique allows one to sweep resonance curves and to determine shifts in resonance frequency.

Piezoelectric Readout

Piezoelectric cantilevers [16.27] are actuated by applying an electric AC voltage via the inverse piezoelectric effect (self-excitation) to the piezoelectric material (PZT or ZnO). Sensing of bending is performed by recording the piezoelectric current change due to the fact that the PZT layer may produce a sensitive field response to weak stress through the direct piezoelectric effect. Such cantilevers are multilayer structures consisting of an SiO_2 cantilever and the PZT piezoelectric layer. Two electrode layers, insulated from each other, provide electrical contact. The entire structure is protected using passivation layers (Fig. 16.7b). An identical structure is usually integrated into the rigid chip body to provide a reference for the piezoelectric signals from the cantilever.

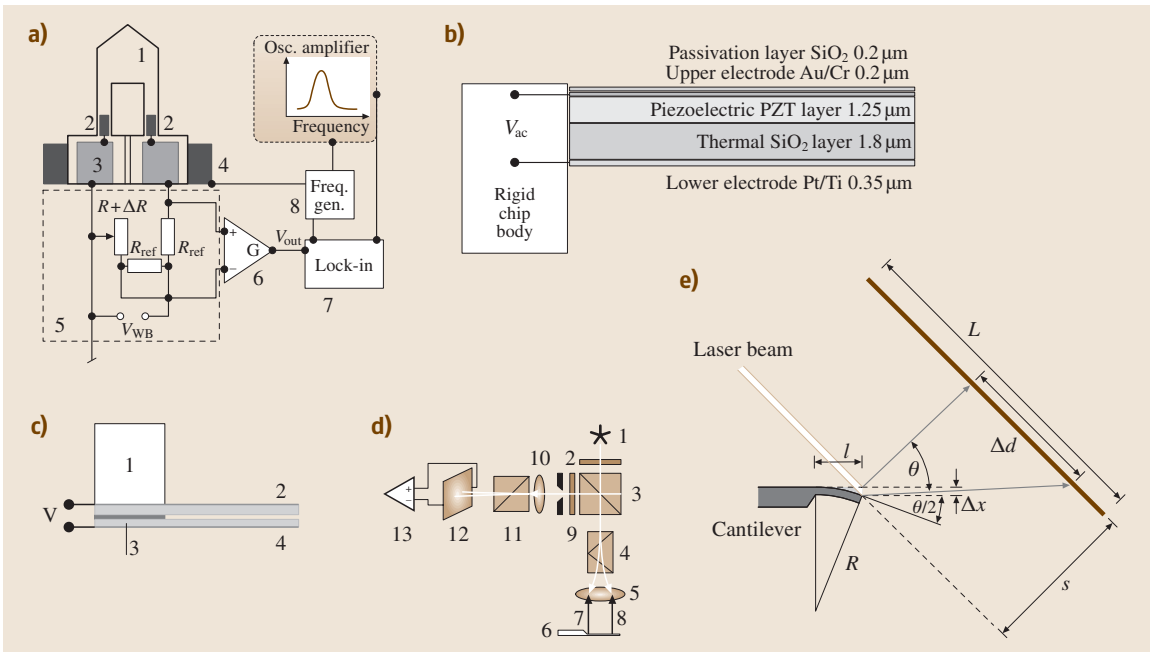

Fig. 16.7 **(a)** Piezoresistive readout: (1) cantilever, (2) piezoresistors, (3) Au contact pads, (4) external piezocrystal for actuation, (5) Wheatstone-bridge circuit, (6) differential amplifier, (7) lock-in amplifier, (8) function generator. **(b)** Piezoelectric readout. **(c)** Capacitive readout: (1) solid support, (2) rigid beam with counter-electrode, (3) insulation layer (SiO_2), (4) flexible cantilever with electrode. **(d)** Interferometric readout: (1) laser diode, (2) polarizer, (3) nonpolarizing beam splitter, (4) Wollaston prism, (5) focusing lens, (6) cantilever, (7) reference beam (near cantilever hinge), (8) object beam (near cantilever apex), (9) diaphragm and $\lambda/4$ plate, (10) focusing lens, (11) Wollaston prism, (12) quadrant photodiode, (13) differential amplifier. **(e)** Beam-deflection readout

Capacitive Readout

For capacitive readout (Fig. 16.7c), a rigid beam with an electrode mounted on the solid support and a flexible cantilever with another electrode layer are used [16.28, 29]. Both electrodes are insulated from each other. Upon bending of the flexible cantilever the capacitance between the two electrodes changes and allows the deflection of the flexible cantilever to be determined. Both static- and dynamic-mode measurements are possible.

Optical (Interferometric) Readout

Interferometric methods [16.30, 31] are most accurate for the determination of small movements. A laser beam passes through a polarizer plate (polarization 45°) and is partially transmitted by a nonpolarized beam splitter (Fig. 16.7d). The transmitted beam is divided in a Wollaston prism into a reference and an object beam. These mutually orthogonally polarized beams are then focused onto the cantilever. Both beams (the reference beam from the hinge region and the object beam from the apex region of the cantilever) are reflected back to the objective lens, pass the Wollaston prism, where they are recombined into one beam, which is then reflected into the other arm of the interferometer, where after the $\lambda/4$ plate a phase shift of a quarter wavelength between object and reference beam is established. Another Wollaston prism separates the reference and object beams again for analysis with a four-quadrant photodiode. A differential amplifier is used to obtain the cantilever deflection with high accuracy. However, the interferometric set-up is quite bulky and difficult to handle.

Optical (Beam-Deflection) Readout

The most frequently used approach to read out cantilever deflections is optical beam deflection [16.32], because it is a comparatively simple method with an excellent lateral resolution. A schematic of this method is shown in Fig. 16.7e.

The actual cantilever deflection Δx scales with the cantilever dimensions; therefore the surface stress $\Delta\sigma$ in N/m is a convenient quantity to measure and compare cantilever responses. It takes into account the cantilever material properties, such as Poisson's ratio ν, Young's modulus E and the cantilever thickness t. The radius of curvature R of the cantilever is a measure of bending, (16.2). As shown in the drawing in Fig. 16.7e, the actual cantilever displacement Δx is transformed into a displacement Δd on the PSD. The position of a light spot on a PSD is determined by measuring the photocurrents from the two facing electrodes. The movement of the light spot on the linear PSD is calculated from the two currents I_1 and I_2 and the size L of the PSD by

$$\Delta d = \frac{I_1 - I_2}{I_1 + I_2} \cdot \frac{L}{2} \,. \tag{16.11}$$

As all angles are very small, it can be assumed that the bending angle of the cantilever is equal to half of the angle θ of the deflected laser beam, i. e. $\theta/2$. Therefore, the bending angle of the cantilever can be calculated to be

$$\frac{\theta}{2} = \frac{\Delta d}{2s} \,, \tag{16.12}$$

where s is the distance between the PSD and the cantilever. The actual cantilever deflection Δx is calculated from the cantilever length l and the bending angle $\theta/2$ by

$$\Delta x = \frac{\theta/2}{2} \cdot l \,. \tag{16.13}$$

Combination of (16.12) and (16.13) relates the actual cantilever deflection Δx to the PSD signal:

$$\Delta x = \frac{l\Delta d}{4s} \,. \tag{16.14}$$

The relation between the radius of curvature and the deflection angle is

$$\frac{\theta}{2} = \frac{l}{R} \,, \tag{16.15}$$

and after substitution becomes

$$R = \frac{2ls}{\Delta d} \,, \tag{16.16}$$

or $R = \frac{2\Delta x}{l^2}$.

16.6 Functionalization Techniques

16.6.1 General Strategy

To serve as sensors, cantilevers have to be coated with a sensor layer that is either highly specific, i. e. is able to recognize target molecules in a key–lock process, or partially specific, so that the sensor information from several cantilevers yields a pattern that is characteristic of the target molecules.

To provide a platform for specific functionalization, the upper surface of these cantilevers is typically coated with 2 nm of titanium and 20 nm of gold, which yields a reflective surface and an interface for attaching functional groups of probe molecules, e.g. for anchoring molecules with a thiol group to the gold surface of the cantilever. Such thin metal layers are believed not to contribute significantly to bimetallic bending, because the temperature is kept constant.

16.6.2 Functionalization Methods

There are numerous ways to coat a cantilever with material, both simple and more advanced ones. The method of choice should be fast, reproducible, reliable and allow one or both of the surfaces of a cantilever to be coated separately.

Simple Methods

Obvious methods to coat a cantilever are thermal or electron-beam-assisted evaporation of material, electrospray or other standard deposition methods. The disadvantage of these methods is that they only are suitable for coating large areas, but not individual cantilevers in an array, unless shadow masks are used. Such masks need to be accurately aligned to the cantilever structures, which is a time-consuming process.

Other methods to coat cantilevers use manual placement of particles onto the cantilever [16.9, 20, 33–35], which requires skillful handling of tiny samples. Cantilevers can also be coated by directly pipetting solutions of the probe molecules onto the cantilevers [16.36] or by employing air-brush spraying and shadow masks to coat the cantilevers separately [16.37].

All these methods have only limited reproducibility and are very time-consuming if a larger number of cantilever arrays has to be coated.

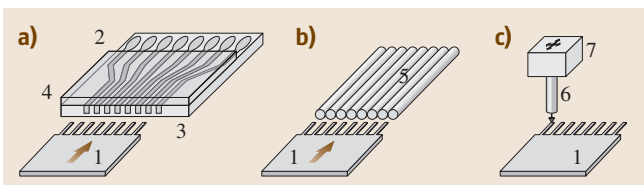

Fig. 16.8 **(a)** Cantilever functionalization in microfluidic networks. **(b)** Incubation in dimension-matched microcapillaries. **(c)** Coating with an inkjet spotter: (1) cantilever array, (2) reservoir wells, (3) microfluidic network with channels, (4) PDMS cover to avoid evaporation, (5) microcapillaries, (6) inkjet nozzle, (7) inkjet *x*-*y*-*z* positioning unit

Microfluidics

Microfluidic networks (μFN) [16.38] are structures of channels and wells, etched several ten to hundred micrometer deep into silicon wafers. The wells can be filled easily using a laboratory pipette, so that the fluid with the probe molecules for coating the cantilever is guided through the channels towards openings at a pitch matched to the distance between individual cantilevers in the array (Fig. 16.8a).

The cantilever array is then introduced into the open channels of the μFN that are filled with a solution of the probe molecules. The incubation of the cantilever array in the channels of the μFN takes from a few seconds (self-assembly of alkanethiol monolayers) to several tens of minutes (coating with protein solutions). To prevent evaporation of the solutions, the channels are covered by a slice of poly(dimethylsiloxane) (PDMS). In addition, the microfluidic network may be placed in an environment filled with saturated vapor of the solvent used for the probe molecules.

Array of Dimension-matched Capillaries

A similar approach is insertion of the cantilever array into an array of dimension-matched disposable glass capillaries. The outer diameter of the glass capillaries is 240 μm so that they can be placed neatly next to each other to accommodate the pitch of the cantilevers in the array (250 μm). Their inner diameter is 150 μm, providing sufficient room to insert the cantilevers (width: 100 μm) safely (Fig. 16.8b). This method has been successfully applied for the deposition of a variety of materials onto cantilevers, such as polymer solutions [16.37], self-assembled monolayers [16.39], thiol-functionalized single-stranded DNA oligonucleotides [16.40], and protein solutions [16.41].

Inkjet Spotting

All of the above techniques require manual alignment of the cantilever array and functionalization tool, and are therefore not ideal for coating a large number of cantilever arrays. The inkjet-spotting technique, however, allows rapid and reliable coating of cantilever arrays [16.42, 43]. An *x*-*y*-*z* positioning system allows a fine nozzle (capillary diameter: 70 μm) to be positioned with an accuracy of approximately 10 μm over a cantilever. Individual droplets (diameter: 60–80 μm, volume 0.1–0.3 nl) can be dispensed individually by means of a piezo-driven ejection system in the inkjet nozzle. When the droplets are spotted with a pitch smaller than 0.1 mm, they merge and form continuous films. By adjusting the number of

droplets deposited on the cantilevers, the resulting film thickness can be controlled precisely. The inkjet-spotting technique allows a cantilever to be coated within seconds and yields very homogeneous, reproducibly deposited layers of well-controlled thickness. Successful coating of self-assembled alkanethiol monolayers, polymer solutions, self-assembled DNA single-stranded oligonucleotides [16.43], and protein layers has been demonstrated. In conclusion, inkjet spotting has turned out to be a very efficient and versatile method for functionalization, which can even be used to coat arbitrarily shaped sensors reproducibly and reliably [16.44, 45].

16.7 Applications

In recent years the field of cantilever sensors has been very active, as the bar chart in Fig. 16.9 of the number of publications between 1993 and 2004 on microcantilevers, cantilever sensors and cantilever arrays demonstrates. This section gives a short overview of the research topics in the field of microcantilever sensors in the literature. Early reports involve the adsorption of alkyl thiols on gold [16.13, 46], detection of mercury vapor and relative humidity [16.47], dye molecules [16.34], monoclonal antibodies [16.48], sugar and proteins [16.49], solvent vapors [16.36, 37, 50, 51], fragrance vapors [16.52] as well as the pH-dependent response of carboxy-terminated alkyl thiols [16.39], label-free DNA hybridization detection [16.17, 40], and biomolecular recognition of proteins relevant in cardiovascular diseases [16.41]. The more recent literature is reviewed in [16.53–56]. Major topics published in 2003 and 2004 include the following studies: fabrication of silicon, piezoresistive [16.57, 58] or polymer [16.59] cantilevers, detection of vapors and volatile compounds, e.g. mercury vapor [16.60], HF vapor [16.61, 62], chemical vapors [16.63], as well as the development of gas sensors utilizing the piezoresistive method [16.64]. Pd-based sensors for hydrogen [16.65], deuterium and tritium [16.66] are reported, as well as sensors based on hydrogels [16.67] or zeolites [16.68]. A humidity sensor is suggested in [16.69]. Further topics include the detection of explosives [16.70], pathogens [16.71], nerve agents [16.72], viruses [16.73], bacteria, e.g. *E. coli* [16.74], and pesticides such as dichlorodiphenyltrichloroethane(DDT) [16.75]. The

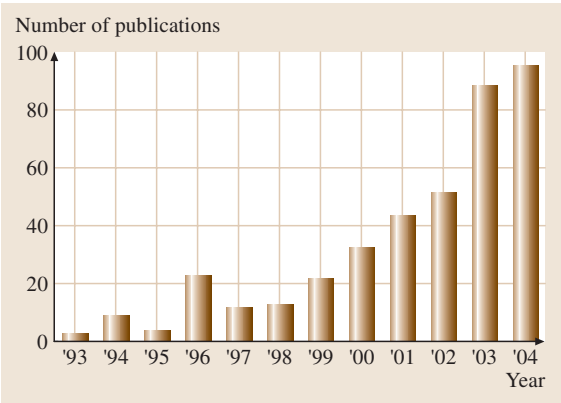

Fig. 16.9 Number of publications from 1993 to 2004 in the field of microcantilevers, cantilever sensors and cantilever arrays

issues of detection of environmental pollutants are discussed in [16.76]. A chemical-vapor sensor based on the bimetal technique is described in [16.77]. Also electrochemical redox reactions have been measured with cantilevers [16.78]. In biochemical applications, detection of DNA [16.18, 79], proteins [16.80], prostate-specific antigen (PSA) [16.81], peptides using antibodies [16.82] and living cells [16.83] has been reported. Medical applications include diagnostics [16.84], drug discovery [16.85], and detection of glucose [16.86]. To increase the complexity of microcantilever applications, two-dimensional microcantilever arrays have been proposed for multiplexed biomolecular analysis [16.87, 88].

16.8 Conclusions and Outlook

Cantilever-sensor array techniques have turned out to be a very powerful and highly sensitive tool to study physisorption and chemisorption processes, as well as to determine material-specific properties such as heat transfer during phase transitions. Experiments in liquids have provided new insights into such complex biochem-

ical reactions as the hybridization of DNA or molecular recognition in antibody–antigen systems or proteomics. Future developments must go towards technological applications, in particular to find new ways to characterize real-world samples such as clinical samples. The development of medical diagnosis tools requires an improvement of the sensitivity of a large number of genetic tests to be performed with small amounts of single donor-blood or body-fluid samples at low cost. From a scientific point of view, the challenge lies in optimizing cantilever sensors to improve their sensitivity to the ultimate limit: the detection of individual molecules.

References

16.1 G. Binnig, C. F. Quate, Ch. Gerber: Atomic force microscope, Phys. Rev. Lett. **56**, 930–933 (1986)

16.2 R. J. Wilfinger, P. H. Bardell, D. S. Chhabra: The resonistor, a frequency sensitive device utilizing the mechanical resonance of a silicon substrate, IBM J. **12**, 113–118 (1968)

16.3 T. M. S. Heng: Trimming of microstrip circuits utilizing microcantilever air gaps, IEEE Trans. Microw. Theory Technol. **19**, 652–654 (1971)

16.4 K. E. Petersen: Micromechanical membrane switches on silicon, IBM J. Res. Dev. **23**, 376–385 (1979)

16.5 E. S. Kolesar: Electronic Nerve Agent Detector, US Patent 4,549,427 (1983)

16.6 T. Itoh, T. Suga: Force sensing microcantilever using sputtered zinc-oxide thin-film, Appl. Phys. Lett. **64**, 37–39 (1994)

16.7 J. P. Cleveland, S. Manne, D. Bocek, P. K. Hansma: A nondestructive method for determining the spring constant of cantilevers for scanning force microscopy, Rev. Sci. Instrum. **64**, 403–405 (1993)

16.8 T. Thundat, R. J. Warmack, G. Y. Chen, D. P. Allison: Thermal, ambient-induced deflections of scanning force microscope cantilevers, Appl. Phys. Lett. **64**, 2894–2896 (1994)

16.9 J. K. Gimzewski, Ch. Gerber, E. Meyer, R. R. Schlittler: Observation of a chemical reaction using a micromechanical sensor, Chem. Phys. Lett. **217**, 589–594 (1994)

16.10 T. Thundat, G. Y. Chen, R. J. Warmack, D. P. Allison, E. A. Wachter: Vapor detection using resonating microcantilevers, Anal. Chem. **67**, 519–521 (1995)

16.11 H. P. Lang, R. Berger, C. Andreoli, J. Brugger, M. Despont, P. Vettiger, Ch. Gerber, J. K. Gimzewski, J.-P. Ramseyer, E. Meyer, H.-J. Güntherodt: Sequential position readout from arrays of micromechanical cantilever sensors, Appl. Phys. Lett. **72**, 383–385 (1998)

16.12 H. Ibach: Adsorbate-induced surface stress, J. Vac. Sci. Technol. A **12**, 2240–2245 (1994)

16.13 R. Berger, E. Delamarche, H. P. Lang, Ch. Gerber, J. K. Gimzewski, E. Meyer, H.-J. Güntherodt: Surface stress in the self-assembly of alkanethiols on gold, Science **276**, 2021–2024 (1997)

16.14 J. R. Barnes, R. J. Stephenson, M. E. Welland, Ch. Gerber, J. K. Gimzewski: Photothermal spectroscopy with femtojoule sensitivity based on micromechanics, Nature **372**, 79–81 (1994)

16.15 G. G. Stoney: The tension of metallic films deposited by electrolysis, Proc. R. Soc. London **82**, 172–177 (1909)

16.16 F. J. von Preissig: Applicability of the classical curvature-stress relation for thin films on plate substrates, J. Appl. Phys. **66**, 4262–4268 (1989)

16.17 J. Fritz, M. K. Baller, H. P. Lang, H. Rothuizen, P. Vettiger, E. Meyer, H.-J. Güntherodt, Ch. Gerber, J. K. Gimzewski: Translating biomolecular recognition into nanomechanics, Science **288**, 316–318 (2000)

16.18 M. Alvarez, L. G. Carrascosa, M. Moreno, A. Calle, A. Zaballos, L. M. Lechuga, C.-A. Martinez, J. Tamayo: Nanomechanics of the formation of DNA self-assembled monolayers, hybridization on microcantilevers, Langmuir **20**, 9663–9668 (2004)

16.19 D. Sarid: *Scanning Force Microscopy with Applications to Electric, Magnetic, and Atomic Forces* (Oxford Univ. Press, New York 1991)

16.20 R. Berger, H. P. Lang, Ch. Gerber, J. K. Gimzewski, J. H. Fabian, L. Scandella, E. Meyer, H.-J. Güntherodt: Micromechanical thermogravimetry, Chem. Phys. Lett. **294**, 363–369 (1998)

16.21 J. E. Sader: Frequency response of cantilever beams immersed in viscous fluids with applications to the atomic force microscope, J. Appl. Phys. **84**, 64–76 (1998)

16.22 T. Bachels, F. Tiefenbacher, R. Schafer: Condensation of isolated metal clusters studied with a calorimeter, J. Chem. Phys. **110**, 10008–10015 (1999)

16.23 J. R. Barnes, R. J. Stephenson, C. N. Woodburn, S. J. O'Shea, M. E. Welland, T. Rayment, J. K. Gimzewski, Ch. Gerber: A femtojoule calorimeter using micromechanical sensors, Rev. Sci. Instrum. **65**, 3793–3798 (1994)

16.24 T. A. Brunt, T. Rayment, S. J. O'Shea, M. E. Welland: Measuring the surface stresses in an electrochemically deposited monolayer: Pb on Au(111), Langmuir **12**, 5942–5946 (1996)

16.25 R. Puers, D. Lapadatu: Electrostatic forces and their effects on capacitive mechanical sensors, Sens. Actuators A **56**, 203–210 (1996)

16.26 J. Fricke, C. Obermaier: Cantilever beam accelerometer based on surface micromachining technology, J. Micromech. Microeng. **3**, 190–192 (1993)
16.27 C. Lee, T. Itoh, T. Ohashi, R. Maeda, T. Suga: Development of a piezoelectric self-excitation, self-detection mechanism in PZT microcantilevers for dynamic scanning force microscopy in liquid, J. Vac. Sci. Technol. B **15**, 1559–1563 (1997)
16.28 T. Göddenhenrich, H. Lemke, U. Hartmann, C. Heiden: Force microscope with capacitive displacement detection, J. Vac. Sci. Technol. A **8**, 383–387 (1990)
16.29 J. Brugger, R. A. Buser, N. F. de Rooij: Micromachined atomic force microprobe with integrated capacitive read-out, J. Micromech. Microeng. **2**, 218–220 (1992)
16.30 C. Schönenberger, S. F. Alvarado: A differential interferometer for force microscopy, Rev. Sci. Instrum. **60**, 3131–3134 (1989)
16.31 M. J. Cunningham, S. T. Cheng, W. W. Clegg: A differential interferometer for scanning force microscopy, Meas. Sci. Technol. **5**, 1350–1254 (1994)
16.32 G. Meyer, N. M. Amer: Novel optical approach to atomic force microscopy, Appl. Phys. Lett. **53**, 2400–2402 (1988)
16.33 R. Berger, Ch. Gerber, J. K. Gimzewski, E. Meyer, H.-J. Güntherodt: Thermal analysis using a micromechanical calorimeter, Appl. Phys. Lett. **69**, 40–42 (1996)
16.34 L. Scandella, G. Binder, T. Mezzacasa, J. Gobrecht, R. Berger, H. P. Lang, Ch. Gerber, J. K. Gimzewski, J. H. Koegler, J. C. Jansen: Combination of single crystal zeolites and microfabrication: Two applications towards zeolite nanodevices, Microporous Mesoporous Mater. **21**, 403–409 (1998)
16.35 R. Berger, Ch. Gerber, H. P. Lang, J. K. Gimzewski: Micromechanics: a toolbox for femtoscale science: towards a laboratory on a tip, Microelectron. Eng. **35**, 373–379 (1997)
16.36 H. P. Lang, R. Berger, F. M. Battiston, J.-P. Ramseyer, E. Meyer, C. Andreoli, J. Brugger, P. Vettiger, M. Despont, T. Mezzacasa, L. Scandella, H.-J. Güntherodt, Ch. Gerber, J. K. Gimzewski: A chemical sensor based on a micromechanical cantilever array for the identification of gases and vapors, Appl. Phys. A **66**, 61–64 (1998)
16.37 M. K. Baller, H. P. Lang, J. Fritz, Ch. Gerber, J. K. Gimzewski, U. Drechsler, H. Rothuizen, M. Despont, P. Vettiger, F. M. Battiston, J.-P. Ramseyer, P. Fornaro, E. Meyer, H.-J. Güntherodt: A cantilever array based artificial nose, Ultramicroscopy **82**, 1–9 (2000)
16.38 S. Cesaro-Tadic, G. Dernick, D. Juncker, G. Buurman, H. Kropshofer, B. Michel, C. Fattinger, E. Delamarche: High-sensitivity miniaturized immunoassays for tumor necrosis factor α using microfluidic systems, Lab on a Chip **4**, 563–569 (2004)
16.39 J. Fritz, M. K. Baller, H. P. Lang, T. Strunz, E. Meyer, H.-J. Güntherodt, E. Delamarche, Ch. Gerber, J. K. Gimzewski: Stress at the solid-liquid interface of self-assembled monolayers on gold investigated with a nanomechanical sensor, Langmuir **16**, 9694–9696 (2000)
16.40 R. McKendry, J. Zhang, Y. Arntz, T. Strunz, M. Hegner, H. P. Lang, M. K. Baller, U. Certa, E. Meyer, H.-J. Güntherodt, Ch. Gerber: Multiple label-free biodetection and quantitative DNA-binding assays on a nanomechanical cantilever array, Proc. Nat. Acad. Sci. USA **99**, 9783–9787 (2002)
16.41 Y. Arntz, J. D. Seelig, H. P. Lang, J. Zhang, P. Hunziker, J.-P. Ramseyer, E. Meyer, M. Hegner, Ch. Gerber: Label-free protein assay based on a nanomechanical cantilever array, Nanotechnology **14**, 86–90 (2003)
16.42 A. Bietsch, M. Hegner, H. P. Lang, Ch. Gerber: Inkjet deposition of alkanethiolate monolayers and DNA oligonucleotides on gold: evaluation of spot uniformity by wet etching, Langmuir **20**, 5119–5122 (2004)
16.43 A. Bietsch, J. Zhang, M. Hegner, H. P. Lang, Ch. Gerber: Rapid functionalization of cantilever array sensors by inkjet printing, Nanotechnology **15**, 873–880 (2004)
16.44 D. Lange, C. Hagleitner, A. Hierlemann, O. Brand, H. Baltes: Complementary metal oxide semiconductor cantilever arrays on a single chip: mass-sensitive detection of volatile organic compounds, Anal. Chem. **74**, 3084–3085 (2002)
16.45 C. A. Savran, T. P. Burg, J. Fritz, S. R. Manalis: Microfabricated mechanical biosensor with inherently differential readout, Appl. Phys. Lett. **83**, 1659–1661 (2003)
16.46 R. Berger, E. Delamarche, H. P. Lang, Ch. Gerber, J. K. Gimzewski, E. Meyer, H.-J. Güntherodt: Surface stress in the self-assembly of alkanethiols on gold probed by a force microscopy technique, Appl. Phys. A **66**, 55 (1998)
16.47 E. A. Wachter, T. Thundat: Micromechanical sensors for chemical and physical measurements, Rev. Sci. Instrum. **66**, 3662–3667 (1995)
16.48 R. Raiteri, G. Nelles, H. J. Butt, W. Knoll, P. Skladal: Sensing of biological substances based on the bending of microfabricated cantilevers, Sens. Actuators B **61**, 213–217 (1999)
16.49 A. M. Moulin, S. J. O'Shea, M. E. Welland: Microcantilever-based biosensors, Ultramicroscopy **82**, 23–31 (2000)
16.50 G. G. Bumbu, G. Kircher, M. Wolkenhauer, R. Berger, J. S. Gutmann: Synthesis and characterization of polymer brushes on micromechanical cantilevers, Macromol. Chem. Phys. **205**, 1713–1720 (2004)
16.51 H. P. Lang, M. K. Baller, R. Berger, Ch. Gerber, J. K. Gimzewski, F. M. Battiston, P. Fornaro, J. P. Ramseyer, E. Meyer, H.-J. Güntherodt: An ar-

tificial nose based on a micromechanical cantilever array, Anal. Chim. Acta **393**, 59–65 (1999)
16.52 F. M. Battiston, J.-P. Ramseyer, H. P. Lang, M. K. Baller, Ch. Gerber, J. K. Gimzewski, E. Meyer, H.-J. Güntherodt: A chemical sensor based on a microfabricated cantilever array with simultaneous resonance-frequency and bending readout, Sens. Actuators B **77**, 122–131 (2001)
16.53 C. Ziegler: Cantilever-based biosensors, Anal. Bioanal. Chem. **379**, 946–959 (2004)
16.54 N. V. Lavrik, M. J. Sepaniak, P. G. Datskos: Cantilever transducers as a platform for chemical and biological sensors, Rev. Sci. Instrum. **75**, 2229–2253 (2004)
16.55 A. Majumdar: Bioassays based on molecular nanomechanics, Dis. Markers **18**, 167–174 (2002)
16.56 H. P. Lang, M. Hegner, Ch. Gerber: Cantilever array sensors, Mater. Today **8**, 30–36 (2005)
16.57 Y. J. Tang, J. Fang, X. D. Yan, H. F. Ji: Fabrication, characterization of SiO_2 microcantilever for microsensor applicatio, Sens. Actuators B **97**, 109–113 (2004)
16.58 E. Forsen, S. G. Nilsson, P. Carlberg, G. Abadal, F. Perez-Murano, J. Esteve, J. Montserrat, E. Figueras, F. Campabadal, J. Verd, L. Montelius, N. Barniol, A. Boisen: Fabrication of cantilever based mass sensors integrated with CMOS using direct write laser lithography on resist, Nanotechnology **15**, 628 (2004)
16.59 A. W. McFarland, M. A. Poggi, L. A. Bottomley, J. S. Colton: Production and characterization of polymer microcantilevers, Rev. Sci. Instrum. **75**, 2756–2758 (2004)
16.60 B. Rogers, L. Manning, M. Jones, T. Sulchek, K. Murray, B. Beneschott, J. D. Adams, Z. Hu, T. Thundat, H. Cavazos, S. C. Minne: Mercury vapor detection with a self-sensing, resonating piezoelectric cantilever, Rev. Sci. Instrum. **74**, 4899–4901 (2003)
16.61 J. Mertens, E. Finot, M. H. Nadal, V. Eyraud, O. Heintz, E. Bourillot: Detection of gas trace of hydrofluoric acid using microcantileve, Sens. Actuators B. **99**, 58–65 (2004)
16.62 Y. J. Tang, J. Fang, X. H. Xu, H. F. Ji, G. M. Brown, T. Thundat: Detection of femtomolar concentrations of HF using an SiO_2 microcantilever, Anal. Chem. **76**, 2478–2481 (2004)
16.63 N. Abedinov, C. Popov, Z. Yordanov, T. Ivanov, T. Gotszalk, P. Grabiec, W. Kulisch, I. W. Rangelow, D. Filenko, Y. J. Shirshov: Chemical recognition based on micromachined silicon cantilever array, Vac. Sci. Technol. B **21**, 2931–2936 (2003)
16.64 J. Zhou, P. Li, S. Zhang, Y. P. Huang, P. Y. Yang, M. H. Bao, G. Ruan: Self-excited piezoelectric microcantilever for gas detection, Microelectron. Eng. **69**, 37–46 (2003)
16.65 D. R. Baselt, B. Fruhberger, E. Klaassen, S. Cemalovic, C. L. Britton Jr., S. V. Patel, T. E. Mlsna, D. McCorkle, B. Warmack: Design and performance of a microcantilever-based hydrogen sensor, Sens. Actuators B **88**, 120–131 (2003)
16.66 A. Fabre, E. Finot, J. Demoment, S. Contreras: Monitoring the chemical changes in Pd induced by hydrogen absorption using microcantilevers, Ultramicroscopy **97**, 425–432 (2003)
16.67 Y. F. Zhang, H. F. Ji, G. M. Brown, T. Thundat: Detection of CrO_4^{2-} using a hydrogel swelling microcantilever sensor, Anal. Chem. **75**, 4773–4777 (2003)
16.68 J. Zhou, P. Li, S. Zhang, Y. C. Long, F. Zhou, Y. P. Huang, P. Y. Yang, M. H. Bao: Zeolite-modified microcantilever gas sensor for indoor air quality control, Sens. Actuators B **94**, 337–342 (2003)
16.69 C. Y. Lee, G. B. Lee: Micromachine-based humidity sensors with integrated temperature sensors for signal drift compensation, J. Micromech. Microeng. **13**, 620–627 (2003)
16.70 L. A. Pinnaduwage, A. Wig, D. L. Hedden, A. Gehl, D. Yi, T. Thundat, R. T. Lareau: Detection of trinitrotoluene via deflagration on a microcantilever, J. Appl. Phys. **95**, 5871–5875 (2004)
16.71 B. L. Weeks, J. Camarero, A. Noy, A. E. Miller, L. Stanker, J. J. De Yoreo: A microcantilever-based pathogen detector, Scanning **25**, 297–299 (2003)
16.72 Y. M. Yang, H. F. Ji, T. Thundat: Nerve agents detection using a Cu^{2+}/L-cysteine bilayer-coated microcantilever, J. Am. Chem. Soc. **125**, 1124–1125 (2003)
16.73 R. L. Gunter, W. G. Delinger, K. Manygoats, A. Kooser, T. L. Porter: Viral detection using an embedded piezoresistive microcantilever sensor, Sens. Actuators A **107**, 219–224 (2003)
16.74 K. Y. Gfeller, N. Nugaeva, M. Hegner: Micromechanical oscillators as rapid biosensor for the detection of active growth of Escherichia coli, Biosens. Bioelectron. **21**, 528–533 (2005)
16.75 M. Alvarez, A. Calle, J. Tamayo, L. M. Lechuga, A. Abad, A. Montoya: Development of nanomechanical biosensors for detection of the pesticide DD, Biosens. Bioelectron. **18**, 649–653 (2003)
16.76 S. Cherian, R. K. Gupta, B. C. Mullin, T. Thundat: Detection of heavy metal ions using protein-functionalized microcantilever sensors, Biosens. Bioelectron. **19**, 411–416 (2003)
16.77 J. D. Adams, G. Parrott, C. Bauer, T. Sant, L. Manning, M. Jones, B. Rogers, D. McCorkle, T. L. Ferrell: Nanowatt chemical vapor detection with a self-sensing, piezoelectric microcantilever array, Appl. Phys. Lett. **83**, 3428–3430 (2003)
16.78 F. Quist, V. Tabard-Cossa, A. Badia: Nanomechanical cantilever motion generated by a surface-confined redox reaction, J. Phys. Chem. B **107**, 10691–10695 (2003)
16.79 R. L. Gunter, R. Zhine, W. G. Delinger, K. Manygoats, A. Kooser, T. L. Porter: Investigation of DNA sensing using piezoresistive microcantilever probes, IEEE Sens. J. **4**, 430–433 (2004)

16.80 J. H. Lee, T. S. Kim, K. H. Yoon: Effect of mass and stress on resonant frequency shift of functionalized $Pb(Zr_{0.52}Ti_{0.48})O_3$ thin film microcantilever for the detection of C-reactive protein, Appl. Phys. Lett. **84**, 3187–3189 (2004)

16.81 G. Wu, R. H. Datar, K. M. Hansen, T. Thundat, R. J. Cote, A. Majumdar: Bioassay of prostate-specific antigen (PSA) using microcantilevers, Nature Biotechnol. **19**, 856–860 (2001)

16.82 B. H. Kim, O. Mader, U. Weimar, R. Brock, D. P. Kern: Detection of antibody peptide interaction using microcantilevers as surface stress sensors, J. Vac. Sci. Technol. B. **21**, 1472–1475 (2003)

16.83 M. T. A. Saif, C. R. Sager, S. Coyer: Functionalized biomicroelectromechanical systems sensors for force response study at local adhesion sites of single living cells on substrates, Annals Biomed. Eng. **31**, 950–961 (2003)

16.84 S. Kumar, R. P. Bajpai, L. M. Bharadwaj: Microcantilever based diagnostic chip for multiple analytes, IETE Techn. Rev. **20**, 361–368 (2003)

16.85 Y. F. Zhang, S. P. Venkatachalan, H. Xu, X. H. Xu, P. Joshi, H. F. Ji, M. Schulte: Micromechanical measurement of membrane receptor binding for label-free drug discovery, Biosens. Bioelectron. **19**, 1473–1478 (2004)

16.86 J. H. Pei, F. Tian, T. Thundat: Glucose biosensor based on the microcantilever, Anal. Chem. **76**, 292–297 (2004)

16.87 K. Khanafer, A. R. A. Khaled, K. Vafai: Spatial optimization of an array of aligned microcantilever based sensors, J. Micromech. Microeng. **14**, 1328–1336 (2004)

16.88 M. Yue, H. Lin, D. E. Dedrick, S. Satyanarayana, A. Majumdar, A. S. Bedekar, J. W. Jenkins, S. Sundaram: A 2-D microcantilever array for multiplexed biomolecular analysis, J. Microelectromech. Syst. **13**, 290–299 (2004)